Contents lists available at ScienceDirect

Free Radical Biology and Medicine

journal homepage: www.elsevier.com/locate/freeradbiomed

Original Contribution

Chloroquine-induced glioma cells death is associated with mitochondrial membrane potential loss, but not oxidative stress

Alexandre Teixeira Vessoni [a], Annabel Quinet [a], Leonardo Carmo de Andrade-Lima [a], Davi Jardim Martins [a], Camila Carrião Machado Garcia [b], Clarissa Ribeiro Reily Rocha [a], Debora Braga Vieira [a], Carlos Frederico Martins Menck [a,*]

[a] Departamento de Microbiologia, Instituto de Ciências Biomédicas, Universidade de São Paulo, Avenida Professor Lineu Prestes, 1374, 05508-000 São Paulo, SP, Brazil
[b] Núcleo de Pesquisa em Ciências Biológicas & Departamento de Ciências Biológicas, Instituto de Ciências Exatas e Biológicas, Universidade Federal de Ouro Preto, Campus Morro do Cruzeiro, Ouro Preto, 35400-000 Minas Gerais, MG, Brazil

ARTICLE INFO

ABSTRACT

Chloroquine (CQ), a quinolone derivative widely used to treat and prevent malaria, has been shown to exert a potent adjuvant effect when combined with conventional glioblastoma therapy. Despite inducing lysosome destabilization and activating p53 in human glioma cells, the mechanisms underlying cell death induced by this drug are poorly understood. Here, we analyzed in a time- and dose-dependent manner, the effects of CQ upon mitochondria integrity, autophagy regulation and redox processes in four human glioma cell lines that differ in their resistance to this drug. NAC-containing media protected cells against CQ-induced loss of mitochondrial membrane potential (MMP), autophagic vacuoles (LC3II) accumulation and loss of cell viability induced by CQ. However, we noticed that part of this protection was due to media acidification in NAC preparations, alerting for problems in experimental procedures using NAC. The results indicate that although CQ induces accumulation of LC3II, mitochondria, and oxidative stress, neither of these events is clearly correlated to cell death induced by this drug. The only event elicited in all cell lines at equitoxic doses of CQ was the loss of MMP, indicating that mitochondrial stability is important for cells resistance to this drug. Finally, the data indicate that higher steady-state MMP values can predict cell resistance to CQ treatment.

© 2015 Elsevier Inc. All rights reserved.

1. Introduction

In the United States, there are 20.59 cases of primary brain and central nervous system (CNS) tumors per 100,000 individuals per year [1], and gliomas account for 80% of these malignant tumors [2]. Gliomas are classified according to their cell type of origin (astrocytoma, oligodendroma or ependymoma) and their brain infiltration capacity [2,3]. According to the WHO, glioblastoma multiforme (GBM), the most malignant and common astrocytoma, is classified as a grade IV astrocytoma (very aggressive and with greater fatality compared with other lower grade, less aggressive

gliomas) [4]. Characteristics of GBM include tissue necrosis, highly proliferative and invasive cells, and pronounced angiogenesis [3,4]. GBM can originate through de novo pathway (no evidence of prior symptoms and usually affecting patients 45 years old or older), or through a progressive pathway (patients usually younger than 45) in which GBM originates from the progressive transformation of lower grade gliomas [3,5].

GBM treatment includes surgical resection, chemotherapy with alkylating and chloroethylating agents (such as temozolomide and carmustine), and radiotherapy [6]. The "gold standard" protocol includes surgical resection followed by combined radiation and temozolomide treatment [7]. However, despite an aggressive multimodal therapy, the median patient survival time is only 12–15 months. Therefore, an understanding of GBM tumor and cell biology is urgently needed to identify new potential therapeutic approaches.

Chloroquine (CQ), a lysosomotropic drug widely used in malaria treatment, has been shown to improve the median survival time of patients undergoing conventional glioblastoma therapy. Patients who received CQ in addition to therapy had a mean

survival time of 27 months, compared with 11 months for patients in the control group [8,9].

At the cellular level, CQ was shown to cause lysosome membrane permeabilization, and is therefore widely used to block autophagy, a lysosome-dependent degradation pathway that has been implicated in the resistance of cancer cells to chemo and radiotherapy possibly through the recycling of damaged and/or superfluous proteins and organelles, such as dysfunctional mitochondria, whose accumulation can be toxic to cells [10–14]. Recent investigation *in vitro* on glioma cells revealed that CQ causes the accumulation of unprocessed autophagic vacuoles (AVs), with the subsequent release of cathepsins into the cytosol, followed by the activation of p53 and caspase-3 [15,16]. In this sense, p53-mutated cells were show to be resistant to CQ-mediated cell death [16]. CQ was also shown to cause oxidative stress. Accordingly, co-treatment of NAC, a widely used antioxidant that acts as precursor of glutathione, was shown to prevent CQ-mediated glutathione depletion and redox imbalance [17]. Given the clinical potential already demonstrated by CQ in GBM therapy [8,9], a better understanding of the mechanisms underlying CQ toxicity and resistance in human glioma cells may help to design new and more effective treatments.

In this sense, we investigated the molecular mechanisms and kinetics of glioma cells' responses to CQ by performing a time-dependent and comparative analysis of mitochondrial accumulation, the alteration of mitochondrial membrane potential (MMP), blockage of autophagy, generation of reactive oxygen species (ROS) and DNA damage and fragmentation between four glioma cell lines that differ in their sensitivity to CQ. We show that MMP loss, but not ROS induction, correlated to cell's susceptibility to equitoxic doses of CQ, and that increased steady-state MMP levels could predict cells resistance to CQ. Interestingly, we also show that culture media acidification is an important component driving NAC-mediated protection against CQ, and that raising pH values of NAC-containing media compromised, but not completely abolished, this effect. Altogether, the results point to an important ROS scavenging-independent mechanism regulating NAC-mediated protection against CQ, and also that the ability of glioma cells to hold MMP values, but not necessarily to control ROS generation, determines cells fate upon CQ treatment.

2. Material and methods

2.1. Cell culture

U87MG, U343MG, U138MG and U251MG glioma cell lines were grown in DMEM (LGC Biotecnologia, Cotia, SP, Brazil) with 10% FBS (Cultilab, Campinas, SP, Brazil) and 1% penicillin/streptomycin (Life Technologies, Carlsbad, CA, USA) at 37 °C in a humidified 5% CO_2 atmosphere. All cell lines were described previously [18,19].

2.2. Drug treatment

Approximately 3.75×10^5, 1.25×10^5 or 2×10^4 cells were plated in 60-mm, 35-mm or 24-well plates, respectively (TPP, Techno Plastic Products, Trasadingen, Zollstrasse, Switzerland). After 24 h, a stock solution of chloroquine diphosphate (CQ) (Sigma-Aldrich, St. Louis, Missouri, USA) (10 mM) was prepared in MilliQ water, filter-sterilized and diluted to the desired concentrations in regular media. For N-acetyl ʟ-cysteine (NAC) (Sigma-Aldrich) treatment, a 40 mM stock solution was prepared by dissolving NAC in DMEM, filter-sterilized, diluted to the desired concentration in regular culture media. CQ was added after NAC working solution was fully prepared. The pH of the stock solution was clearly acid and pH was measured immediately after dissolving this drug in DMEM

(pH=4.2). To evaluate the effects of pH on cell treatment, the pH was adjusted (with NaOH 1 M) to DMEM regular values (pH=7.6). Culture media with low pH (in the absence of NAC) was prepared by reducing the pH (with HCl 6 M). Both solutions were processed similarly in order to prepare working solutions (10% FBS and 1% antibiotics) and the pH values, immediately before adding to cells, were 6.6 for 25 mM NAC, 6.6 for "low pH media", 7.6 for "normal pH NAC", and 7.6 for regular culture media.

2.3. Cell viability test (XTT), Sub-G1 and γ-H2AX analysis by flow cytometry

Cells were washed with PBS and incubated with XTT labeling mixture for approximately 50 min, according to the manufacturer's instructions (Cell Proliferation Kit II XTT, Roche, Basel, Switzerland). Sub-G1 DNA and γ-H2AX content were analyzed as previously described [20]. Briefly, both adherent and detached cells were fixed with 1% formaldehyde for 15 min on ice, washed with PBS, fixed with 70% ethanol (Labsynth, Diadema, SP, Brazil), and stored at −20 °C. Prior to analysis, cells were blocked and permeabilized with 0.2% Triton X-100 (Sigma-Aldrich) in PBS and 1% BSA, then incubated with anti-γ-H2AX (Anti-phospho-Histone H2AX [ser139], clone JBW301, Upstate, Millipore, Billerica, MA, USA) and anti-mouse FITC (Sigma-Aldrich) antibodies. DNA was stained using 20 mg/ml propidium iodide (PI) (Calbiochem, Merck, Whitehouse Station, NJ, USA), 0.02 mg/ml RNase A (Life Technologies) and 0.1% Triton X-100 solution. PI (red) and γ-H2AX (green) fluorescence were measured by flow cytometry (Guava Easycyte, Millipore).

2.4. Western blot analysis

Cells were lysed in 50 mM Tris pH 7.5, 20 mM NaCl, 1 mM $MgCl_2$, 0.1% SDS (Sigma-Aldrich), 1 mM Na_3VO_4, protease inhibitor cocktail (Cocktail Set III, Calbiochem) and 0.25 units/ml benzonase (Novagen, Merck). After quantification (Bradford method, Bio-Rad Laboratories, Hercules, CA, USA), the proteins were separated on an SDS–polyacrylamide gel and blotted onto a nitrocellulose transfer membrane (GE Healthcare, Waukesha, WI, USA). Protein expression was detected using anti-LC3 (Sigma-Aldrich), anti-tubulin, anti-GAPDH or anti-TOM20 (Santa Cruz, Santa Cruz, CA, USA), anti-p62 (Cell Signaling) or anti-cleaved PARP (Abcam, Cambridge, MA, USA) antibodies. A chemiluminescent HRP substrate (Millipore) was used to develop the membranes, and the luminescence intensity was determined using an ImageQuant 300 (GE Healthcare).

2.5. MitoTracker analysis

Mitochondrial content was determined using the MitoTracker® Red FM Probe (Life Technologies) according to the manufacturer's instructions, with modifications. Briefly, cells were incubated with 50 nM MitoTracker Red in regular media for 40 min, detached with trypsin (Adolfo Lutz Institute, São Paulo, SP, Brazil), resuspended in 1% FBS DMEM without phenol red, and the mean red fluorescence intensity was measured by flow cytometry.

2.6. Mitochondrial membrane potential (MMP) analysis

MMP variation was determined as previously described [21], with modifications. Cells were detached with trypsin and incubated for 15 min with 50 nM tetramethylrhodamine, methyl ester perchlorate (TMRM) (Life Technologies) in PBS containing 0.1% FBS. After washing, the cells were resuspended in PBS (0.1% FBS), and the mean yellow fluorescence intensity was measured by flow cytometry.

2.7. Analysis of reactive oxygen species (ROS) generation

ROS levels were analyzed as previously described [22]. Briefly, cells were detached with trypsin and incubated for 30 min with 10 μM of DCFDA (2′,7′-dichlorofluorescein diacetate, Sigma-Aldrich, 35845), or for 15 min with 5 μM of Mitosox (Life Technologies, M36008) in DMEM containing 0.2% FBS and without phenol red. The mean green or red fluorescence intensity was measured by flow cytometry. Hydrogen peroxide (1 mM) and actinomycin D (10 μM) were used as positive controls for DCFDA and Mitosox analysis, respectively.

2.8. DNA isolation and quantitative long PCR for DNA damage analysis

Cells were lysed using 1% SDS and 100 μg/ml proteinase K (Sigma-Aldrich), and DNA was isolated after phenol:chloroform:isoamyl alcohol extraction (1 volume) followed by 100% ethanol precipitation (2.5 volumes). DNA was quantitated with a Quant-iT dsDNA Picogreen kit (Invitrogen, Life Technologies) using a Glo-Max Microplate Multimode Fluorometer (Promega, Fitchburg, MA, USA) with a Blue Optical Kit filter (*Ex*: 490 nm, *Em*: 510–570 nM) (Promega). As previously described [23], 15 ng DNA was used for qPCR using TaKaRa LA PCR (TaKaRa Bio Group, Japan). The parameters were 85 °C hot start addition of DNA polymerase; cycles: 94 °C for 3 min; 29–31 cycles of 94 °C for 30 s; 69 °C for 9 min; 4 °C infinity. The PCR products were run on a 0.7% agarose gel and quantitated using a Quant-iT dsDNA Picogreen kit. The analysis was performed by calculating the ratio of the corrected values of fluorescence in the irradiated samples divided by that of the non-irradiated sample. The negative natural logarithm ($-\ln$) of this ratio was calculated to determine the frequency of lesions per fragment based on a Poisson distribution and assuming that DNA damage is randomly distributed across the genome. Supplementary Table S1 provides detailed information about primers, gene length and amplified locus size.

2.9. Alkaline comet assay

The alkaline comet assay was performed as previously described [20] with modifications for the detection of oxidized purines with the *Escherichia coli* Formamido Pyrimidine–DNA Glycosylase (FPG) [24]. Briefly, after overnight lysis, the comet slides were washed in FPG glycosylase buffer (40 mM Hepes pH 7, 10 mM MgCl$_2$, 1 mM DTT), and incubated for 30 min at 37 °C with FPG (New England Biolabs, Ipswich, MA, USA) at 8 U/ml in $1 \times$ NEB-uffer 1, supplemented with 100 μg/ml BSA (both supplied by the manufacturer). One half of each slide was incubated with the enzyme, while the other half was incubated with the same solution, but without the glycosylase (negative control). Experiments were performed in duplicate and twice independently. Comets were stained with ethidium bromide, imaged with a fluorescence microscope (Olympus BX51, Olympus, Center Valley, PA, USA), and at least 50 comets were scored for each condition per slide with Kinetic Imaging Komet 6.0 (Andor™ Technology, Belfast, UK).

2.10. Mitochondrial (mt) DNA copy number analysis

20 ng of DNA was isolated using DNeasy Blood & Tissue Kit (QIAGEN), and submitted to a quantitative PCR reaction using the SYBR green probe, in a 7500 Real Time equipment (Life Technologies). The ratio of mtDNA (as evidence by ND1 gene amplification) to nuclear DNA (HPRT gene amplification) was used to estimate mtDNA amount per cell. Primers used were HPRT sense: TGACATGTGCCGCCTGCGAG; HPRT reverse: GTGGTCGCTTTCC GTGCCGA; ND1 sense: ACTACGCAAAGGCCCCAACG; ND1 reverse:

GAGCTAAGGTCGGGGCGGTG.

2.11. Statistical analysis

Statistical significance was assessed using unpaired test, one-way ANOVA or two-way ANOVA followed by the Bonferroni test (Prism 5, GraphPad Software Inc.).

3. Results

3.1. Time course analysis of CQ-induced alterations in U87MG cells

We first investigated the time-dependent mitochondrial alterations, oxidative stress (ROS levels) and the accumulation of AVs (LC3II, as a readout for autophagy impairment) in U87MG glioma cells exposed to 50 μM CQ. This dose reduces cell viability to approximately 10–20% after 48 h of continuous treatment (Fig. 1A), as measured by the Cell Proliferation Kit II (XTT). Cell viability of the glioma cell lines U343MG, U138MG and U251MG is also shown in Fig. 1A. Since this assay measures conversion of XTT to formazan by mitochondria, cell viability is used as a direct measure of mitochondrial metabolic activity. By staining mitochondria with MitoTracker (a probe capable of staining mitochondria regardless the polarization status of this organelle [25]), we noticed, by flow cytometry, a continuous increase in the content of these organelles over time (Fig. 1B). Conversely, by staining cells with TMRM, a cell-permeable cationic dye whose accumulation in the mitochondria is driven by their membrane potential, we observed, also by flow cytometry, an early and progressive loss of MMP in the presence of CQ (Fig. 1C). The generation of ROS was measured by incubating cells with DCFDA or MitoSox probes. The use of MitoSox revealed that the formation of mitochondrial superoxide occurs at early time points (Fig. 1D). In contrast, DCFDA revealed ROS induction only at later time points (48 h) of CQ treatment (Fig. 1E). Representative histograms of flow cytometry analyses (MitoTracker, TMRM, DCFDA and Mitosox) are shown in Supplementary Fig. S1. Finally, the accumulation of LC3II is evident as early as 1 h post-CQ treatment (Fig. 1F). This was accompanied by an accumulation of TOM20 (a mitochondrial translocase receptor located in the outer membrane of the mitochondria) confirming the increase in organelle levels over continuous CQ treatment, starting as early as 1 h post CQ treatment (Fig. 1F). However, we could not detect any increase in mitochondrial DNA (mtDNA) copy number in CQ-treated cells (Fig. 1G). Therefore, results suggest that CQ results in the accumulation of swollen (increased TOM20 and mitotracker staining) and dysfunctional (reduced MMP and increased mitosox staining) mitochondria, but not organelle biogenesis (Fig. 1G). In summary, we observed that CQ induced LC3II and mitochondrial accumulation, loss of MMP and mitochondrial superoxide generation are detectable at the very first hours of treatment with CQ, and these effects increased in a time-dependent manner. Interestingly, ROS detection by DCFDA probe was only observable at a later time point.

3.2. NAC and culture media acidification protects glioma cells from CQ toxicity

We then investigated the effects of NAC, a widely used anti-oxidant, on U87MG cells co-treated with CQ. Results show that NAC drastically reduced CQ-induced loss of cell viability and MMP, DNA fragmentation, PARP cleavage, and AVS accumulation (as measured by LC3II and p62 accumulation) (Fig. 2). We also allowed cells to recover for an additional 72 h in complete media after CQ and/or NAC treatment, and analyzed them under a light
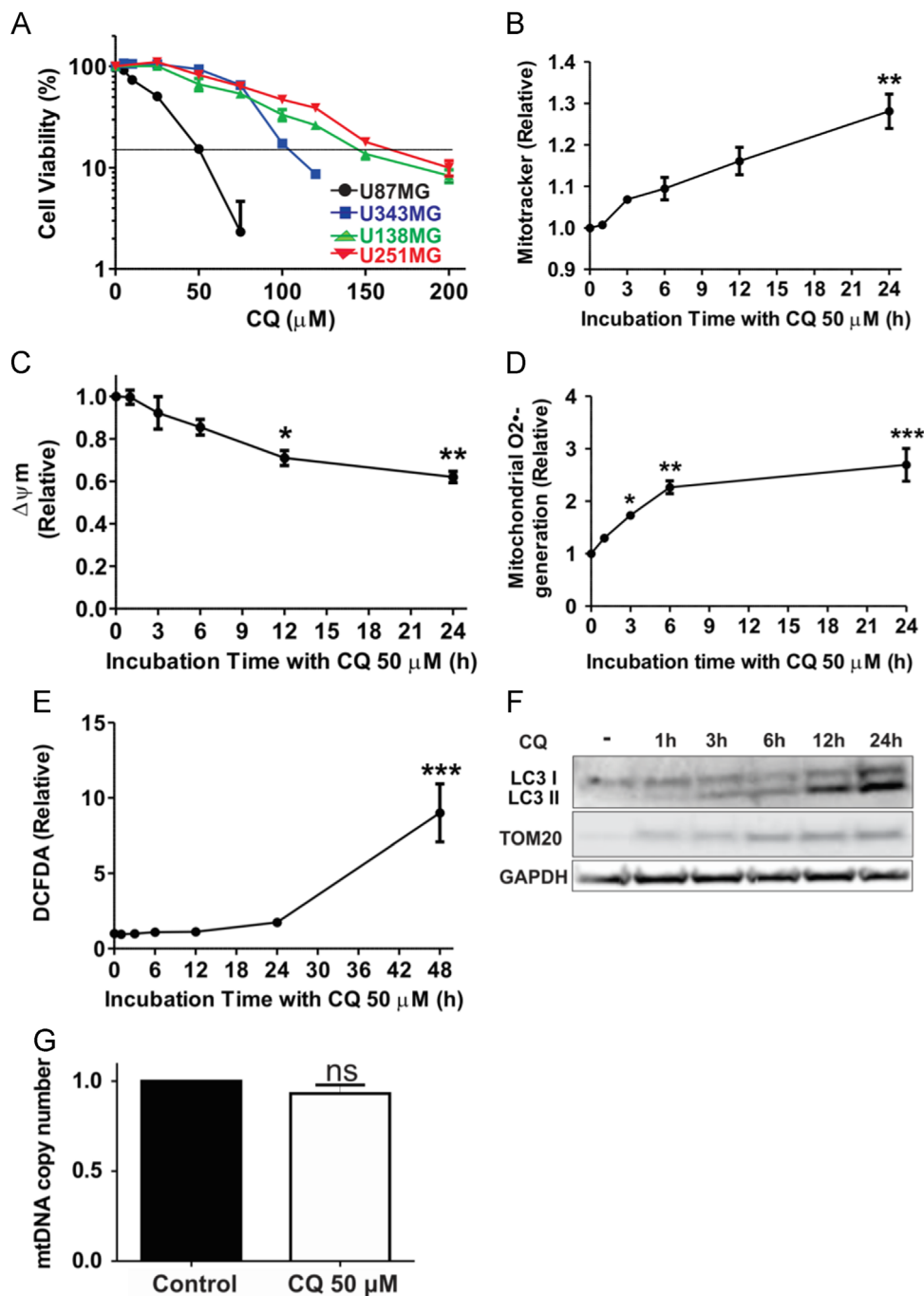
Fig. 1. Time-dependent analysis of CQ toxicity in U87MG cells. (A) Cell viability (XTT Cell Viability Assay II) after 48 h of treatment with different doses of CQ in U87MG, U343MG, U138MG and U251MG glioma cell lines (line evidences 15% of survival). (B) Time-dependent accumulation of mitochondria (measured by MitoTracker staining) induced by 50 μM CQ. (C) Time-dependent alterations in mitochondrial membrane potential (MMP) induced by 50 μM CQ (TMRM staining). (D) Time-dependent mitochondrial superoxide (O2•−) formation induced by 50 μM CQ (Mitosox staining). (E) Time-dependent generation of ROS induced by 50 μM CQ (measured by DCFCDA). (F) Time-dependent accumulation of LC3II and of Tom20 induced by 50 μM CQ. (G) mitochondrial DNA (mtDNA) copy number quantification (expressed as ND1 relative to HPRT gene copies) of cells treated for 24 h with 50 μM CQ. $^{*}\,p < 0.05$, $^{**}\,p < 0.01$ and $^{***}\,p < 0.001$.

microscope (Fig. 2B). Representative pictures show that NAC protected cells from CQ toxicity, in strong contrast to cells treated only with CQ, in which only sparse cells remained attached to the plate. Therefore, results show that NAC prevents not only CQ-induced cell death, but also the onset of early events induced by CQ. The protective effect of NAC was also observed in the U343MG, U138MG and U251MG cells (Supplementary Fig. S2).

Since NAC causes acidification of the culture media (see Section 2 for details), and that CQ loses its ability to diffuse across cell membrane once it is protonated [26], we asked whether the

protective effects of NAC could be attributed to alterations in the pH during treatment. Therefore, we compared cell viability, MMP loss and LC3II accumulation upon CQ treatment in the presence of culture media supplemented with 25 mM of NAC ("NAC", pH=6.6); culture media with lower pH ("low pH media", pH=6.6); or culture media supplemented with 25 mM of NAC with pH equivalent to regular media solution value ("normal pH NAC", pH=7.7). Interestingly, solely acidification of the culture media exerted a potent and significant protection against CQ toxicity, reduction on LC3II and MMP loss, similar to the same
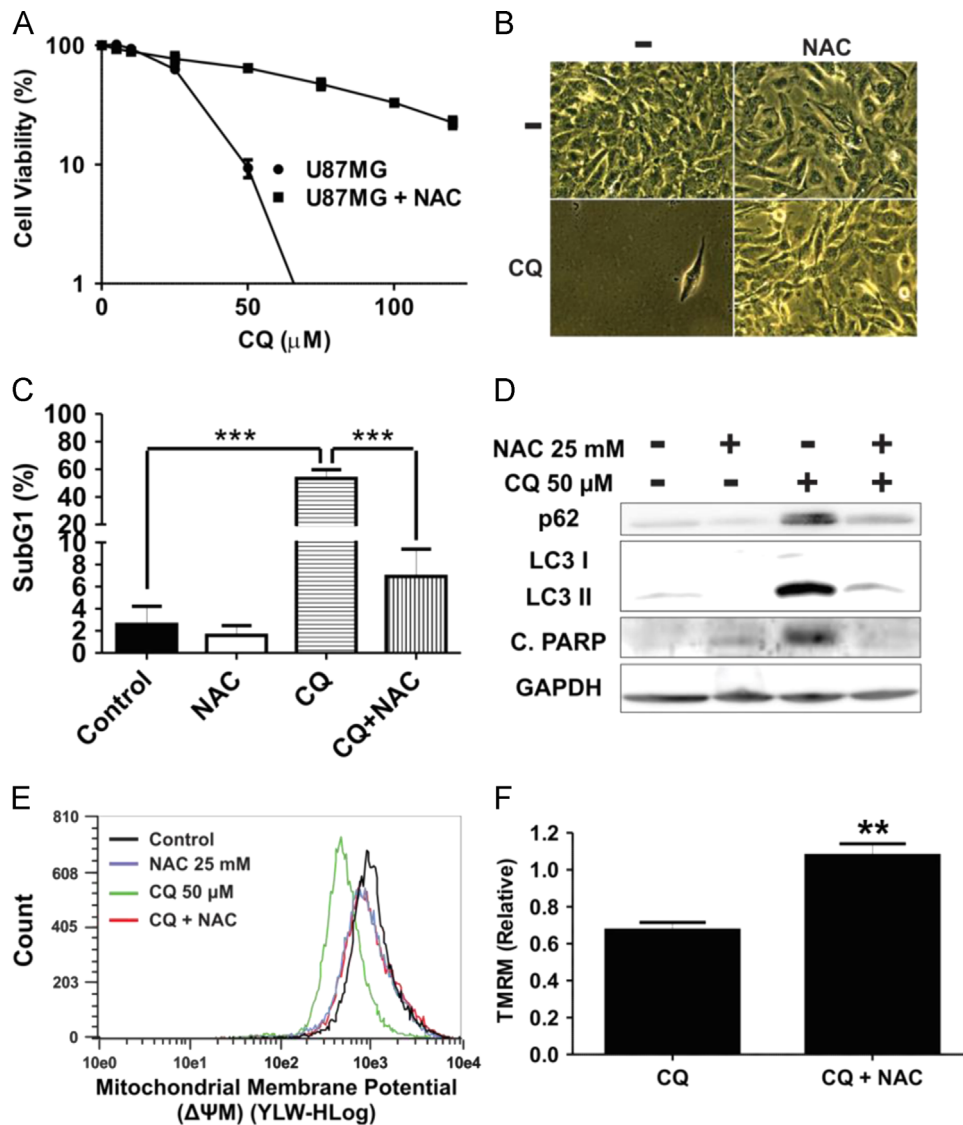
Fig. 2. NAC protects U87MG from CQ-induced cytotoxicity. (A) Cell viability analysis (XTT) of U87MG cells after a 48 h co-treatment with NAC (25 mM) and CQ (different doses). (B) Glioma cells analyzed under a light microscope after 48 h of treatment with CQ (50 μM) and/or NAC, followed by an additional 72 h of culture on regular media with no drugs. (C) Analysis of Sub-G1 formation (by flow cytometry) induced by 48 h of treatment with 50 μM of CQ and/or 25 mM of NAC. (D) LC3II, p62 and cleaved PARP expression analyzed by western blotting in glioma cells treated with 25 μM of CQ and/or 25 mM of NAC for 24 h. (D–F) Mitochondrial membrane potential ($\Delta\psi m$) alterations induced by 24 h of treatment with 50 μM of CQ and/or 25 mM of NAC (fold change of CQ-treated/untreated). ** $p < 0.01$, *** $p < 0.001$.

medium containing NAC (Fig. 3). However, the protective effects of NAC were still observed in CQ-treated cells when pH value is adjusted. The results show that, in fact, lowering pH in cultured media is enough to exert a potent protective effect against CQ toxicity, and careful analyses must be taken when testing NAC in these types of experiment.

3.3. Glioma cells' sensitivity to CQ correlates with MMP loss, but not ROS generation

To better understand the mechanisms that drive resistance of glioma cells to CQ, the cytotoxic effects of CQ were investigated in three other human glioma cell lines, comparing the accumulation of AVs and of mitochondria, ROS generation and MMP alterations. Because these cells differ in the resistance to CQ, these experiments were performed both at 50 μM of CQ (common dose to all cell lines), or at equitoxic doses (i.e., capable of reducing cell viability to 10–20% after a 48 h-treatment) based on data obtained by

the XTT assay (Fig. 1A). The equitoxic doses varied between cell lines (50 μM for U87MG, 100 μM for U343MG, and 150 μM for both U138MG and U251MG). Results show that accumulation of mitochondria (Fig. 4A, Supplementary Fig. S1A) and of LC3II (Fig. 4E) occurred in all four cell lines after treatment with both 50 μM and the equitoxic dose of CQ (more pronounced in this case). Interestingly, loss of MMP in the resistant cell lines, on the other hand, was achieved only after treatment with the higher, equitoxic doses (Fig. 4B, Supplementary Fig. S1B). ROS detection by the Mitosox and DCFDA probes also revealed alterations (except for DCFDA detection for U343 cells), but the changes were unrelated to the CQ toxic effects. Interestingly, the cell line U343MG failed to significantly increase ROS levels regardless the dose of CQ used (Fig. 4D and Supplementary Fig. S1D). These results indicate that loss of MMP, but not LC3II/mitochondria accumulation nor ROS generation, is achieved only upon exposure of cells to the equitoxic dose of CQ, presenting a strong correlation with cells sensitivity to CQ.
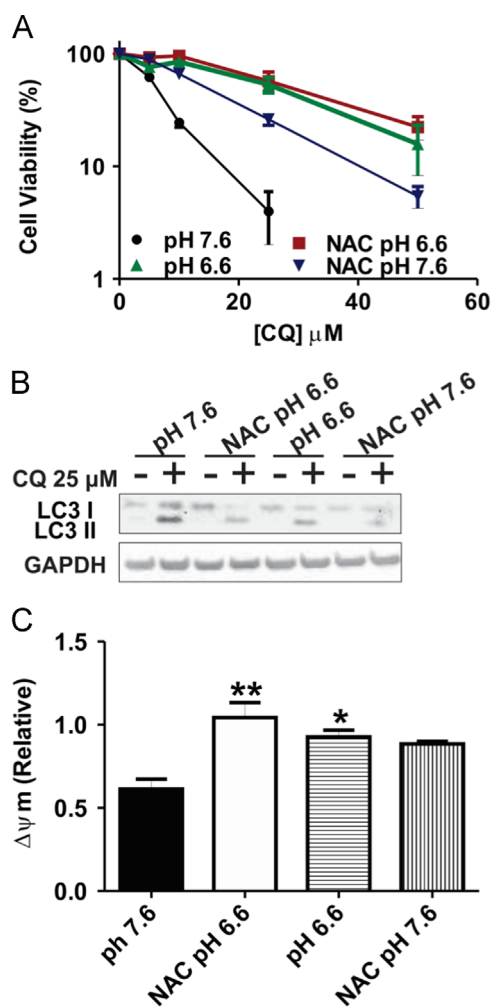
A

B

C

Fig. 3. NAC-induced extracellular acidification prevents CQ toxicity. (A) Cell viability (XTT) analysis of U87MG cells treated for 48 h with different doses of CQ diluted in culture medium with normal pH in the absence of NAC (pH 7.6), normal pH in the presence of NAC (NAC pH 7.6), low pH in the absence of NAC (pH 6.6) or low pH in the presence of NAC (NAC pH 6.6). (NAC=25 mM; normal pH=7.6; low pH=6.6). (B) Accumulation of LC3II in cells treated with 25 μM of CQ and/or NAC (25 mM) upon the effect of normal or low pH. (C) Mitochondrial membrane potential ($\Delta\psi m$) alterations (relative of CQ-treated to untreated) of cells treated with 50 μM of CQ and/or NAC upon the effect of normal or low pH for 24 h.

3.4. Increased steady-state MMP and reduced mitochondrial content in CQ-resistant glioma cells

We next compared the basal levels of mitochondria content, as well as MMP and ROS generation, between all four glioma cell lines. Results show that U87MG cells have significantly more mitochondria content (Fig. 5A), as well as lower MMP (Fig. 5B) than the other resistant cell lines. Interestingly, basal levels of ROS generation, when measured with the DCFDA probe, were higher in the U343MG cells than in the other glioma cell lines (Fig. 5D). On the other hand, mitochondrial superoxide generation, as measured by Mitosox, was not statistically different among the cell lines analyzed, although the U138MG seems to display lower steady-state levels between all cells tested (Fig. 5C). Therefore, we show that cell lines with increased resistance to CQ toxicity have higher steady-state levels of MMP, as well as reduced mitochondrial content, while no clear correlation between basal ROS levels and CQ sensitivity could be drawn based on analyses with neither DCFDA nor Mitosox probes.

3.5. CQ induces purine oxidation, but not DNA strand breaks

Loss of MMP can be elicited in response to DNA damage, activating apoptosis through the intrinsic (mitochondrial) pathway [27]. To investigate the induction of DNA damage in cells treated with CQ, we analyzed the phosphorylation of the histone H2A variant H2AX (γ-H2AX), a commonly used marker for DNA damage, in U87MG cells exposed to 50 μM CQ at different time points (Fig. 6A). We detected a mild increase in γ-H2AX at 48 h post-treatment. This induction of γ-H2AX coincides with an increase in Sub-G1 cell population, possibly representing DNA fragmentation in apoptotic cells (Figs. 2C and 6B). It is important to notice that an increase in Sub-G1 in the cell lines U343MG, U138MG and U251MG could only be observed at the equitoxic doses of CQ (Fig. 6B). To rule out the presence of DNA damage at earlier time points after CQ treatment, we performed an extra long PCR on DNA extracted from U87MG cells that had been treated with 50 μM of CQ for 6 or 24 h. The presence of toxic helix-distorting lesions or DNA strand breaks, which stall polymerases [28,29], would prevent the long PCR reaction from proceeding. We did not observe a significant number of DNA lesions (less than one lesion per 100 kbp) in the cells treated with 50 μM CQ (Fig. 6C, irradiation of cells with 30 J/m² of UVC light was used as a positive control for the presence of DNA damage). These data are consistent with the absence of γ-H2AX formation until 48 h after CQ treatment. We also employed the comet assay under alkaline conditions to detect the presence of strand breaks in the DNA of glioma cells treated with 50 μM of chloroquine during 6 or 24 h (Fig. 6D). This assay was also performed after incubation of the DNA with the FPG glycosylase, which nicks DNA when damaged by several different lesions induced by oxidative stress [24]. We did not observe any significant increase in tail moment in samples not treated with FPG, confirming the absence of strand breaks in the DNA of CQ-treated samples, in agreement with the long PCR results. However, we detected a significant increase in the tail moment of the CQ-treated samples after FPG treatment (treatment of cells with 50 μM of H_2O_2 for 15 min was used as a positive control for FPG activity). Results confirm that chloroquine induces oxidation of purines, but not formation of DNA strand breaks or replication-stalling lesions on the DNA of glioma cells treated with CQ, at time points when MMP is already compromised.

4. Discussion

In this work, mechanisms related to glioma cells resistance to CQ were investigated. We performed a time-dependent analysis of the accumulation of AVs (LC3II) and of mitochondria, reduction of MMP, and the participation of redox processes during CQ treatment of glioma cell lines. Basically, we exposed the cells to doses of CQ that reduce cell viability to approximately 10–20% after 48 h of continuous treatment. Since the cell viability assay used (XTT) reflects mitochondrial enzymatic activity, we also investigated CQ-induced cell death by apoptosis (Sub-G1 induction and PARP cleavage, Fig. 2), and the results confirm that loss of cell viability reflects cell death induction. Second, the data indicate that accumulation of AVs and of mitochondria with reduced MMP occurs during the very first hours of treatment. It is important to emphasize that the probe used to evaluate mitochondria content (Mitotracker Deep Red) remains bound to this organelle regardless its membrane potential. Conversely, the probe used to evaluate mitochondrial membrane potential (TMRM) display weak binding to mitochondria, and its retention on this organelle is strictly dependent on the membrane potential of it [25]. The mechanism behind MMP loss was not evaluated herein, although previous publications shed light on this issue. Lysosome membrane
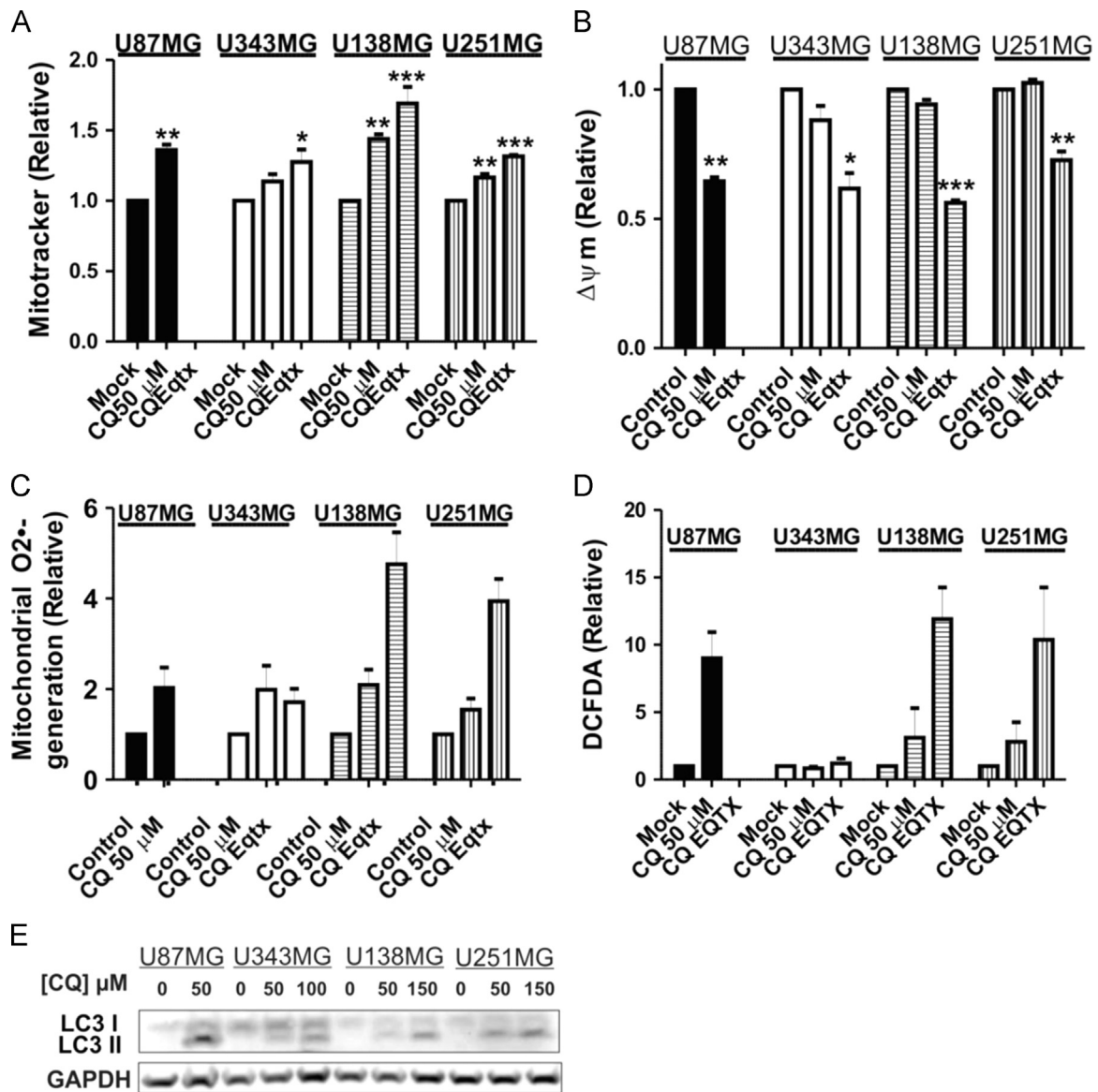
Fig. 4. CQ-resistant human glioma cell lines show increased resistance to lose MMP. Mitochondrial content (A), mitochondrial membrane potential ($\Delta\psi m$) (B), mitochondrial superoxide ($O_2\bullet-$) (C), DCFDA (D) and LC3II levels in human glioma cell lines in response to treatment with 50 μM or with equitoxic (EQTX) doses of CQ (100 μM for U343MG; 150 μM for U138MG and U251MG), determined based on the data obtained by the XTT assay. Analyses were performed after 24 h (A, B, C and E) or 48 h (D) of continuous treatment with CQ. Data was normalized for the untreated (control) for each cell line * $p < 0.05$, ** $p < 0.01$ and *** $p < 0.001$.

permeabilization (LMP) elicited by CQ causes cathepsins B and D release to the cytosol. Both enzymes were shown to cleave Bid, inducing BAX translocation to the mitochondria, followed by cytochrome C release and loss of MMP, thereby connecting LMP to MMP [15,30,31]. ROS generation was detected at these very early time points when the Mitosox probe (which detects mitochondrial superoxide formation) was employed. Accordingly, we detected DNA bases oxidation upon CQ treatment, although no DNA breaks or replication blocking lesions were detected, even when MMP integrity was already compromised. On the other hand, use of DCFDA probe revealed generation of ROS only at later time points. It is important to emphasize that the DCFDA probe is oxidized to a fluorescent form and becomes trapped inside of cells. This oxidation, however, is not due to exposure to ROS in general (such as superoxide), but probably to hydroxyl radicals [32]. Thus, it is plausible that the increased DCF fluorescence we detected at later time points of CQ treatment reflect a late accumulation of hydroxyl radicals, based on conversion of early-formed mitochondrial superoxide to hydrogen peroxide (through superoxide dismutase),

which is further converted to hydroxyl radicals by Fenton-type reactions. Although there is an increase in ROS generation upon CQ treatment, this event was not a good indicator of cell toxicity. For example, in the cell line U343MG, mitochondrial superoxide production showed undistinguishable levels upon treatment with 50 μM (which is barely toxic) or with 100 μM of CQ (which reduces cell viability to approximately 10–20%) (Fig. 4C and Supplementary Fig. S1). For the U138MG cells, although no significant MMP loss was detected upon treatment with 50 μM of CQ (which is also barely toxic for these cells), there was an important induction of mitochondrial superoxide formation to levels comparable to that observed in the U87MG cell line (Fig. 4C). Moreover, use of DCFDA probe provided no evidence of hydroxyl radicals formation in the U343MG cell line, regardless of the CQ doses used (Fig. 4D). From all parameters analyzed, only MMP loss showed a clear correlation to cell viability, where very similar levels of MMP loss were achieved for all cell lines tested upon treatment with an equitoxic dose of CQ (Fig. 4B). In this sense, it is worth pointing out that once MMP loss is achieved, occurs the release of activators of catabolic
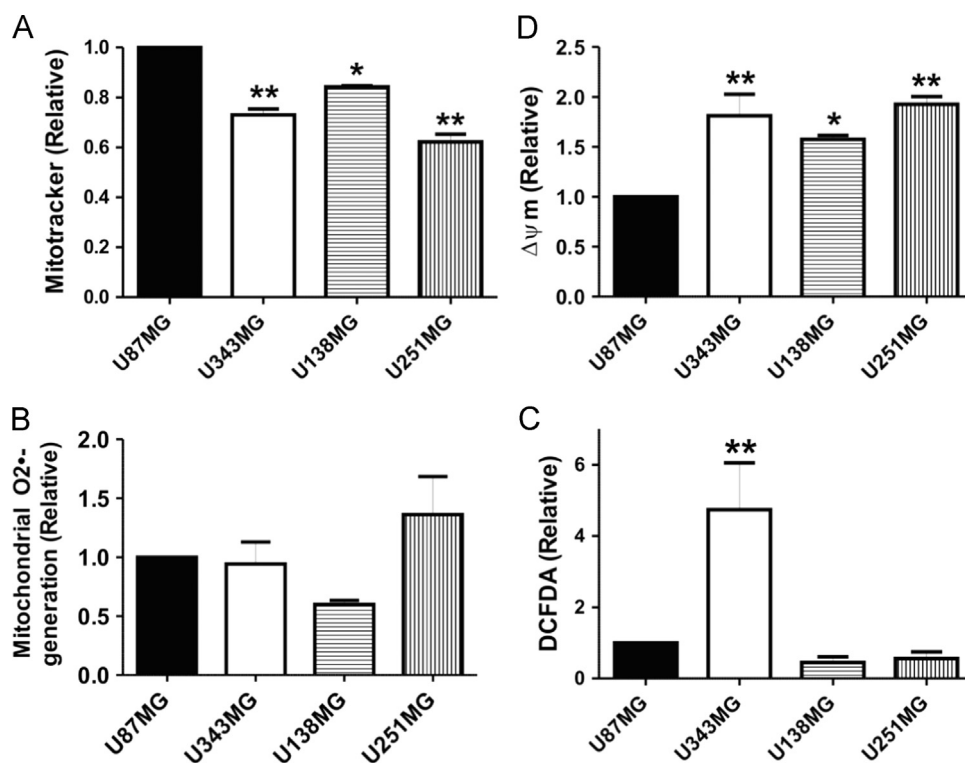
Fig. 5. Steady-state levels of mitochondria content, mitochondria membrane potential ($\Delta\psi m$) and ROS in human glioma cells. Mitochondria content was measured by mitotracker staining (A), $\Delta\psi m$ was measured by TMRM staining (B), and ROS levels were measured by Mitosox (C) and DCFDA (D) probes. A total of 10,000 events were analyzed for all cell lines tested, and data are expressed as relative to U87MG cell line values. * $p < 0.05$, ** $p < 0.01$.

hydrolases (such as caspases), which promotes cell death [33].

We also noticed that U87MG cell line (the most sensitive cell line tested to CQ) exhibit more mitochondrial content and lower MMP at steady-state conditions than the other (and more resistant) cell lines. These results point to a scenario in which cells with more mitochondria and/or with lower MMP are more susceptible to CQ toxicity. In this sense, it is worth pointing out that although U343MG has less mitochondria content and increased MMP than U138MG, it is more sensitive to CQ than the latter (the most resistant among the four cell lines). Since U343MG has a wild type version of the p53 protein, in contrast to U138MG and U251MG cell lines, it is possible that this characteristic renders it more susceptible to the toxic effects of CQ, as previously shown [16]. On the other hand, the mitochondrial features, described herein, of the U343MG cells may render them more resistant to CQ than U87MG cells, also carrying functional p53 protein. Therefore, mitochondria content and MMP, together with p53, should all interplay to determine cells' susceptibility to CQ.

Addition of NAC, a widely used ROS scavenger and glutathione precursor, not only prevented CQ-induced cell death (loss of cell viability, PARP cleavage and Sub-G1 formation), but also abolished loss of MMP and LC3II accumulation (Fig. 2). However, we also noticed that NAC causes acidification of cell media when dissolved on it, and this acidification, by itself, also offered cells protection to CQ treatment. Although the acid effect was observed, NAC preparations where the pH was corrected still offered some cell protection, most likely due to the ability of NAC to increase glutathione levels, therefore preventing an increase in nitric oxide and oxidative stress [17]. Although speculative, it is possible that glutathione may conjugate to CQ, and mediate its efflux out of the cell through multidrug resistant-associated protein located on the plasma membrane, in a similar manner as suggested by Raj and collaborators in their work with CQ-resistant *Plasmodium falciparium* strains [34]. On the other hand, the effects of media acidification are not only something to take care for experimental procedures when working with NAC, but may also have biological relevance. Recently, melanoma, colon carcinoma and osteosarcoma cells cultivated under acidic conditions were shown to have inhibited the CQ ability to block autophagy flux, although the effects on MMP were not evaluated by the authors [35]. It is known that CQ is able to diffuse across cell membrane, and becomes trapped inside acidic compartments (such as lysosomes) once it is protonated, rendering this drug lysosomotropic [26]. Thus, the protective effect elicited by NAC due to culture media acidification is probably a result of protonation of CQ outside of the cells, impairing its translocation and intracellular accumulation. Therefore, these results do not exclude that the protective effect of NAC can be elicited, at least in part, due to an increase in antioxidant defenses, but suggest caution in the interpretation of results during co-treatment of NAC with CQ. It also argues that tumor cells in poor oxygenated areas (displaying a shift to glycolysis with consequent release and accumulation of metabolic acids, promoting acidification of that microenvironment) will not respond to CQ during therapy, as recently discussed by Pellegrini et al. [35]. Therefore, it is possible that CQ may elicit a beneficial effect on glioma treatment by contributing to the loss of MMP induced by radiotherapy [36] and chemotherapy [37] restricted to cancer cells located in non-hypoxic areas of the tumors, where acidification probably does not occur.

Finally, DNA damage as measured by γ-H2AX was only detected at a later time point (48 h) that coincides with Sub-G1 accumulation, and thus is probably related to apoptosis. The long PCR and comet assay techniques confirmed the absence of breaks and replication blocking DNA lesions in glioma cells shortly after CQ treatment, when the loss of MMP and the accumulation of AVs and mitochondria were already detectable. Therefore, these results reinforce the idea that DNA fragmentation does not precede CQ-induced cell death/loss of MMP.
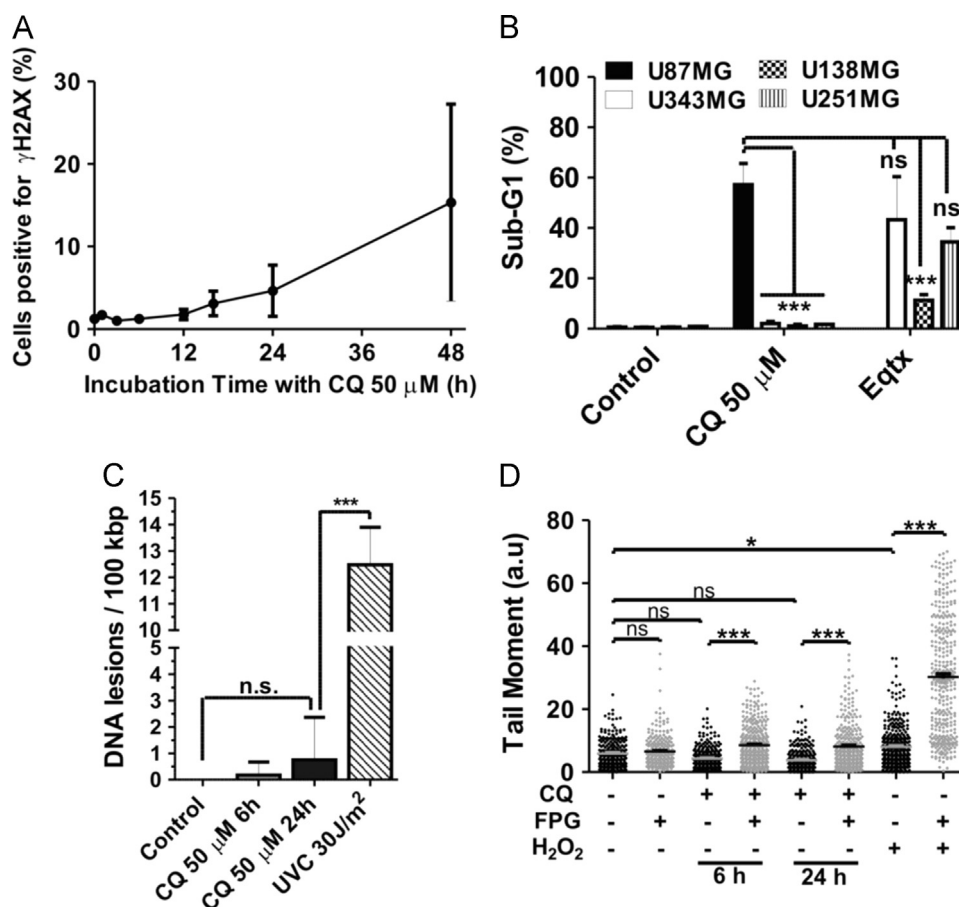
Fig. 6. CQ-induced DNA damage is a late event. (A) DNA damage induction (as measured by γ-H2AX formation through flow cytometry) after a continuous 48 h of treatment with 50 μM of CQ in U87MG cells. (B) Sub-G1 formation after a 48 h treatment with 50 μM or with equitoxic (EQTX) doses of CQ (100 μM for U343MG; 150 μM for U138MG and U251MG), determined based on the data obtained by the XTT assay. (C) Detection of helix-distorting lesions or strand breaks in the DNA of U87MG cells treated with 50 μM CQ for 6 or 24 h, through the quantitative long PCR method (30 J/m^2 of UVC was used as a positive control). (D) Detection of strand breaks by the alkaline comet assay in U87MG cells treated with 50 μM CQ for 6 or 24 h, with or without FPG treatment. *** $p < 0.001$.

Together, the data indicate that p53 status is not the sole responsible for glioma cell resistance to CQ treatment, pointing to an important role for glutathione, autophagy blockage and MMP in the regulation of CQ cytotoxicity in glioma cells. Moreover, since the resistance of different glioma cell lines to CQ is strictly associated to cells' ability to maintain MMP upon stress, but not necessarily to their capacity to control oxidative stress upon CQ treatment, results suggest that glutathione may also interfere in the process of CQ-induced cytotoxicity in a redox control-independent mechanism. Finally, our results suggest that assessing MMP and mitochondria content of surgery-derived tumor cells may help to predict efficacy of adding CQ to conventional GBM therapy.

Conflict of interest

The authors declare that they have no competing interests.

Author's contribution

ATV conceived initial idea, designed and carried out experiments, interpreted data, and drafted the manuscript. AQ designed and carried out experiments, interpreted data, and critically revised the manuscript. LCAL designed and carried out experiments, interpreted data, and critically revised the manuscript. DJM and CRRR carried out experiments. CCMG and DBV carried out experiments, and critically revised the manuscript. CFMM interpreted data, critically revised the manuscript, and conceived initial idea.

Appendix A. Supplementary material

Supplementary data associated with this article can be found in the online version at http://dx.doi.org/10.1016/j.freeradbiomed.

2015.11.008.

References

[1] T.A. Dolecek, J.M. Propp, N.E. Stroup, C. Kruchko, CBTRUS statistical report: primary brain and central nervous system tumors diagnosed in the United States in 2005–2009, Neuro-Oncology (2012).
[2] S. Agnihotri, K. Burrell, A. Wolf, S. Jalali, C. Hawkins, J. Rutka, G. Zadeh, Glioblastoma, a brief review of history, molecular genetics, animal models and novel therapeutic strategies, Arch. Immunol. Ther. Exp. 61 (2013) 25–41.
[3] F. Furnari, T. Fenton, R. Bachoo, A. Mukasa, J. Stommel, A. Stegh, W. Hahn, K. Ligon, D. Louis, C. Brennan, L. Chin, R. DePinho, W. Cavenee, Malignant astrocytic glioma: genetics, biology, and paths to treatment, Genes Dev. 21 (2007) 2683–2710.
[4] D.N. Louis, H. Ohgaki, O.D. Wiestler, W.K. Cavenee, P.C. Burger, A. Jouvet, B. W. Scheithauer, P. Kleihues, The 2007 WHO classification of tumours of the central nervous system, Acta Neuropathol. 114 (2007) 97–109.
[5] H. Ohgaki, P. Kleihues, The definition of primary and secondary glioblastoma, Clin. Cancer Res. 19 (2013) 764–772.
[6] R. Stupp, M. Brada, M.J. van den Bent, J.-C. Tonn, G. Pentheroudakis, High-grade glioma: ESMO Clinical Practice Guidelines for diagnosis, treatment and follow-up, Ann. Oncol.: Off. J. Eur. Soc. Med. Oncol. 25 (Suppl. 3) (2014) iii93–iii101.
[7] R. Stupp, W. Mason, M. van den Bent, M. Weller, B. Fisher, M. Taphoorn, K. Belanger, A. Brandes, C. Marosi, U. Bogdahn, J. Curschmann, R. Janzer, S. Ludwin, T. Gorlia, A. Allgeier, D. Lacombe, G. Cairncross, E. Eisenhauer, R. Mirimanoff, Radiotherapy plus concomitant and adjuvant temozolomide for glioblastoma, N. Engl. J. Med. 352 (2005) 987–996.
[8] J. Sotelo, E. Briceño, M.A. López-González, Adding chloroquine to conventional treatment for glioblastoma multiforme: a randomized, double-blind, placebo-controlled trial, Ann. Intern. Med. 144 (2006) 337–343.
[9] E. Briceño, A. Calderon, J. Sotelo, Institutional experience with chloroquine as an adjuvant to the therapy for glioblastoma multiforme, Surg. Neurol. 67 (2007) 388–391.
[10] Y. Xu, H. Yu, H. Qin, J. Kang, C. Yu, J. Zhong, J. Su, H. Li, L.K. Sun, Inhibition of autophagy enhances cisplatin cytotoxicity through endoplasmic reticulum stress in human cervical cancer cells, Cancer Lett. 314 (2012) 232–243.
[11] X.L. Guo, D. Li, F. Hu, J.R. Song, S.S. Zhang, W.J. Deng, K. Sun, Q.D. Zhao, X.Q. Xie, Y.J. Song, M.C. Wu, L.X. Wei, Targeting autophagy potentiates chemotherapy-induced apoptosis and proliferation inhibition in hepatocarcinoma cells, Cancer Lett. 320 (2012) 171–179.
[12] A. Knizhnik, W. Roos, T. Nikolova, S. Quiros, K. Tomaszowski, M. Christmann, B. Kaina, Survival and death strategies in glioma cells: autophagy, senescence and apoptosis triggered by a single type of temozolomide-induced DNA damage, PLoS One 8 (2013) e55665.
[13] M. Degtyarev, A. De Mazière, C. Orr, J. Lin, B.B. Lee, J.Y. Tien, W.W. Prior, S. Van Dijk, H. Wu, D.C. Gray, D.P. Davis, H.M. Stern, L.J. Murray, K.P. Hoeflich, J. Klumperman, L.S. Friedman, K. Lin, Akt inhibition promotes autophagy and sensitizes PTEN-null tumors to lysosomotropic agents, J. Cell Biol. 183 (2008) 101–116.
[14] B. Ravikumar, Z. Berger, C. Vacher, C. O'Kane, D. Rubinsztein, Rapamycin pre-treatment protects against apoptosis, Hum. Mol. Genet. 15 (2006) 1209–1216.
[15] Y. Geng, L. Kohli, B.J. Klocke, Ka Roth, Chloroquine-induced autophagic vacuole accumulation and cell death in glioma cells is p53 independent, Neuro-Oncology 12 (2010) 473–481.
[16] E. Kim, R. Wu, A. Ru, C. Schmitz-salue, G. Warnecke, E. Bu, N. Pettkus, D. Speidel, W. Schulz-schaeffer, W. Deppert, A. Giese, Chloroquine activates the p53 pathway and induces apoptosis in human glioma cells, Neuro-Oncology 12 (2010) 389–400.
[17] B. Park, S. Park, S. Paek, S. Park, M. Kwak, H. Choi, C. Yong, B. Yoo, J. Kim, Chloroquine-induced nitric oxide increase and cell death is dependent on cellular GSH depletion in A172 human glioblastoma cells, Toxicol. Lett. 178 (2008) 52–60.
[18] L.F.Z. Batista, W.P. Roos, M. Christmann, C.F.M. Menck, B. Kaina, Differential sensitivity of malignant glioma cells to methylating and chloroethylating anticancer drugs: P53 determines the switch by regulating xpc, ddb2,and DNA double-strand breaks, Cancer Res. 67 (2007) 11886–11895.
[19] L. Batista, W. Roos, B. Kaina, C. Menck, p53 mutant human glioma cells are sensitive to UV-C-induced apoptosis due to impaired cyclobutane pyrimidine dimer removal, Mol. Cancer Res. 7 (2009) 237–246.
[20] A. Quinet, A.T. Vessoni, C.R.R. Rocha, V. Gottifredi, D. Biard, A. Sarasin, C.F. M. Menck, A. Stary, Gap-filling and bypass at the replication fork are both active mechanisms for tolerance of low-dose ultraviolet-induced DNA damage in the human genome, DNA Repair 14 (2014) 27–38.
[21] M. Scheibye-Knudsen, M. Ramamoorthy, P. Sykora, S. Maynard, P. Lin, R. Minor, D. Wilson, M. Cooper, R. Spencer, R. de Cabo, D. Croteau, V. Bohr, Cockayne syndrome group B protein prevents the accumulation of damaged mitochondria by promoting mitochondrial autophagy, J. Exp. Med. (2012) 855–869.
[22] K. Asensi, R. Fortunato, D. dos Santos, T. Pacheco, D. de Rezende, D. Rodrigues, F. Mesquita, T. Kasai-Brunswick, A. de Carvalho, D. Carvalho, A. Carvalho, R. Goldenberg, Reprogramming to a pluripotent state modifies mesenchymal stem cell resistance to oxidative stress, J. Cell. Mol. Med. 18 (2014) 824–831.
[23] A.M. Furda, A.S. Bess, J.N. Meyer, B. Van Houten, Analysis of DNA damage and repair in nuclear and mitochondrial DNA of animal cells using quantitative PCR, Methods Mol. Biol. 920 (2012) 111–132.
[24] A.R. Collins, A.A. Oscoz, G. Brunborg, I. Gaivão, L. Giovannelli, M. Kruszewski, C. C. Smith, R. Štětina, The comet assay: topical issues, Mutagenesis 23 (2008) 143–151.
[25] C. Cottet-Rousselle, X. Ronot, X. Leverve, J.F. Mayol, Cytometric assessment of mitochondria using fluorescent probes, Cytometry Part A 79A (2011) 405–425.
[26] V. Solomon, H. Lee, Chloroquine and its analogs: a new promise of an old drug for effective and safe cancer therapies, Eur. J. Pharmacol. 625 (2009) 220–233.
[27] D.R. Green, G. Kroemer, The pathophysiology of mitochondrial cell death, Science 305 (2004) 626–629.
[28] C.J. Rudolph, A.L. Upton, R.G. Lloyd, Replication fork stalling and cell cycle arrest in UV-irradiated Escherichia coli, Genes Dev. 21 (2007) 668–681.
[29] E.R. Edenberg, M. Downey, D. Toczyski, Polymerase stalling during replication, transcription and translation, Curr. Biol. 24 (2014) R445–R452.
[30] H. Appelqvist, A. Johansson, E. Linderoth, U. Johansson, B. Antonsson, R. Steinfeld, K. Kågedal, K. Ollinger, Lysosome-mediated apoptosis is associated with cathepsin D-specific processing of bid at Phe24, Trp48, and Phe183, Ann. Clin. Lab. Sci. 42 (2012) 231–242.
[31] P. Boya, K. Andreau, D. Poncet, N. Zamzami, J.-L. Perfettini, D. Metivier, D. M. Ojcius, M. Jäättelä, G. Kroemer, Lysosomal membrane permeabilization induces cell death in a mitochondrion-dependent fashion, J. Exp. Med. 197 (2003) 1323–1334.
[32] M. Karlsson, T. Kurz, U.T. Brunk, S.E. Nilsson, C.I. Frennesson, What does the commonly used DCF test for oxidative stress really show? Biochem. J. 428 (2010) 183–190.
[33] G. Kroemer, L. Galluzzi, C. Brenner, Mitochondrial membrane permeabilization in cell death, Physiol. Rev. (2007) 99–163.
[34] D. Raj, J. Mu, H. Jiang, J. Kabat, S. Singh, M. Sullivan, M. Fay, T. McCutchan, X. Su, Disruption of a Plasmodium falciparum multidrug resistance-associated protein (PfMRP) alters its fitness and transport of antimalarial drugs and glutathione, J. Biol. Chem. 284 (2009) 7687–7696.
[35] P. Pellegrini, A. Strambi, C. Zipoli, M. Hägg-Olofsson, M. Buoncervello, S. Linder, A. De Milito, Acidic extracellular pH neutralizes the autophagy-inhibiting activity of chloroquine: implications for cancer therapies, Autophagy 10 (2014) 1–10.
[36] J.K. Leach, G. Van Tuyle, P. Lin, R. Schmidt-ullrich, R.B. Mikkelsen, Ionizing radiation-induced, mitochondria-dependent generation of reactive oxygen/nitrogen, Cancer Res. 61 (2001) 3894–3901.
[37] C.-J. Lin, C.-C. Lee, Y.-L. Shih, C.-H. Lin, S.-H. Wang, T.-H. Chen, C.-M. Shih, Inhibition of mitochondria- and endoplasmic reticulum stress-mediated autophagy augments temozolomide-induced apoptosis in glioma cells, PLoS One 7 (2012) e38706.